See published version at: https://doi.org/10.1007/s10571-020-00836-z

Title

Pathway-focused profiling of oligodendrocytes over-expressing miR-125a-3p reveals alteration of Wnt and cell-to-cell signaling

Authors

Davide Marangon, Maria P. Abbracchio*, Davide Lecca*

Department of Pharmacological and Biomolecular Sciences, Università degli Studi di Milano, Via Balzaretti 9, 20133 Milano, Italy.

*Equally contributing

Corresponding author:
Dr. Davide Lecca
Università degli Studi di Milano
Dipartimento di Scienze Farmacologiche e Biomolecolari
Via Balzaretti 9, 20133 Milan, Italy.
Tel: +39 02 50318271
E-mail: davide.lecca@unimi.it

ORCID:
Davide Lecca: https://orcid.org/0000-0002-3258-363X
Davide Marangon: https://orcid.org/0000-0003-2606-8110
Maria P. Abbracchio: https://orcid.org/0000-0002-7833-3388

Acknowledgements

This work was supported by Fondazione Cariplo, grant no. 2014-1207 to DL, by Fondo per il Finanziamento delle Attività Base di Ricerca, FFABR 2017) to DL, by FISM –Fondazione Italiana Sclerosi Multipla - cod. 2017/R/1 and financed or co-financed with the '5 per mille' public funding to MPA, Università degli Studi di Milano (Piano di Sostegno alla Ricerca 2015–17—LINEA 2 and. The funders had no role in study design, data collection and analysis, decision to publish, or preparation of the manuscript.

Compliance with Ethical Standards

The authors declare that they have no conflict of interest.

See published version at: https://doi.org/10.1007/s10571-020-00836-z

This article does not contain any studies with human participants performed by any of the authors.

International (European law Dir. 2010/63/UE) and national (Italian law DL n. 26, 4th March 2014) guidelines for the care and use of animals were followed. All the procedures were approved by the Italian Ministry of Health (735-2015PR to DL).

Abstract

MicroRNAs are small post-transcriptional regulators that modulate gene expression by directly interacting with their target transcripts. Since the interaction between miRNAs and target mRNAs does not require a perfect match, one single miRNA can influence the expression of several genes and lead to a very broad array of functional consequences. Recently, we identified miR-125a-3p as a new regulator of oligodendrocyte development, showing that its over-expression is associated to impaired oligodendrocyte maturation. However, whether and how miR-125a-3p overexpression is causally related to oligodendrocyte maturation is still obscure, as well as the pathways responsible for this effect. To shed light on this issue and to identify the underlying molecular mechanisms, we determined the transcriptomic profile of miR-125a-3p over-expressing oligodendrocytes and, by means of two complementary bioinformatic approaches, we have identified pathways and biological processes consistently modulated by miR-125a-3p alteration. This analysis showed that miR-125a-3p is involved in the regulation of cell-cell interactions and Wnt signaling. By means of pathway-focused PCR arrays, we confirmed that miR-125a-3p induces changes in the expression of several genes encoding for adhesion molecules and gap junctions, which play key roles in oligodendrocytes after exposure to pathological demyelinating stimuli. Moreover, the expression changes of different Wnt targets suggest an over-activation of this pathway. Globally, our studies show that miR-125a-3p over-expression can alter signaling pathways and biological processes essential for myelin formation in oligodendrocytes, suggesting that alteration of miR-125a-3p levels may contribute to impairing oligodendrocyte maturation in demyelinating diseases.

Keywords

Oligodendrocyte, miRNA, gene ontology, pathway analysis

Author Contributions

DM designed and performed in vitro experiments, in silico analysis and qPCR, analysed the data, prepared the figures and wrote the manuscript; MPA contributed to data interpretation and discussion and revised the manuscript. DL supervised the project, designed the experiments and wrote the manuscript. All authors read and approved the final manuscript.

See published version at: https://doi.org/10.1007/s10571-020-00836-z

Introduction

In the central nervous system, oligodendrocytes are specialized glial cells that produce myelin, a lipid structure that surrounds axons ensuring their insulation and the saltatory conduction of nerve impulses. Axon-to-oligodendrocyte signals are essential for physiological myelination and contribute to orchestrate the terminal stages of oligodendrocyte differentiation by regulating the expression of both cell–cell and cell-extracellular matrix adhesion molecules, such as integrins, laminins, contactins and connexins (Laursen et al. 2009). In myelinating glia, gap junctions (GJs) are involved in many physiological processes, including the regulation of cell growth, cell permeability and calcium signaling, and they also play a fundamental role in myelin maintenance (Nualart-Marti et al. 2013).

Oligodendrocyte development is tightly regulated by intrinsic time-dependent mechanisms that control cell proliferation and maturation via signaling cascades, ending with the activation of several factors that can directly modulate gene expression. Among these regulators, microRNAs emerged as pivotal players in the regulation of oligodendrocyte development, both under physiological and pathological conditions (Marangon et al. 2019). MiRNAs control gene expression by binding to complementary sequences in the 3′ untranslated regions of their target messenger RNAs. This interaction does not require perfect complementarity between miRNAs and mRNA sequences; indeed, a 6-base match may be enough to induce mRNA degradation or translational inhibition. This apparently reduces miRNA target specificity, but, on the other hand, it also enables one single miRNA to modulate several biological processes by targeting multiple genes in a shared pathway (Gurtan and Sharp 2013).

In this respect, we recently identified miR-125a-3p as a new regulator of oligodendrocyte maturation, showing that its over-expression decreases the production of the myelin basic protein (MBP), one of the major myelin components (Lecca et al. 2016). Although this former study highlighted the deleterious effect of miR-125a-3p over-expression on OPC maturation, the underlying molecular mechanisms are still unknown. In the present study, we aimed at analysing the transcriptome of oligodendrocytes over-expressing miR-125a-3p taking advantage of two complementary approaches (pathway- and ontology-based), to identify the over-represented signaling pathways and biological processes and, eventually, by means of pathway-focused PCR arrays, to determine the role of miR-125a-3p in their regulation.

Results

MiR-125a-3p over-expression in OPCs inhibits TCF7L2 signaling.

To explore the mechanisms underlying the effects of miR-125a-3p on oligodendrocyte maturation, we performed a transcriptomic analysis of differentiating OPC cultures after miR-125a-3p over-expression. We considered a threshold of ±1.5 fold change and an FDR-adjusted p-values < 0.05 to obtain the list of genes that are differentially expressed in the two experimental conditions (miR-125a-3p transfected OPCs vs. scramble RNA transfected OPCs). This analysis allowed the identification of 1060 genes significantly changed after miR-125a-3p over-expression (Fig. 1).

See published version at: https://doi.org/10.1007/s10571-020-00836-z

The list of the differentially expressed genes was first analysed by means of a pathway-oriented approach. The Ingenuity® Pathway Analysis software (IPA®, QIAGEN) was used to perform an upstream regulator analysis, that allows to identify master regulators of gene expression that may be responsible for the observed changes in the experimental dataset, and to understand whether they are likely activated or inhibited. The analysis showed that miR-125a-3p over-expression can influence the activity of several regulators in OPCs, such as cytokines, growth factors and transcription factors (Table 1). Among the potential candidates, we focused on TCF7L2, an essential effector of the Wnt pathway that can also promote oligodendrocyte maturation in a Wnt-independent manner (Hammond et al. 2015). As suggested by the very low Z score (-5.186), the TCF7L2 signaling was strongly inhibited after miR-125a-3p over-expression. This observation was based on the down-regulation of 27 TCF7L2-related genes in our experimental data set (Fig. 2).

Based on these results, we hypothesized that the over-expression of miR-125a-3p leads to Wnt signaling over-activation, preventing TCF7L2 pro-myelinating Wnt-independent effect. To assess this hypothesis, we utilized the pathway focused "Wnt signaling targets" array that simultaneously allowed to profile the expression of 84 key genes responsive to WNT signal transduction (see Table S1 for the full gene list and fold changes). After miR-125a-3p overexpression, changes were detected in 24 out of 84 genes (Fig. 3a). The 8 down-regulated genes (fold regulation < -1.5) were the following: Fgf7, Nrp1, Mmp2, Sox2, Met, Plaur, Tcf7l1 and Fst. The 16 up-regulated genes (fold regulation > 1.5) were the following: Wisp1, Ctgf, Dlk1, Egr1, Gja1, Cdh1, Wisp2, Klf5, Wnt3a, Igf1, Ptgs2, Abcb1a, Cubn, Fn1, Tcf7, Twist1. The change in the expression levels of the Wnt ligand Wnt3a and Wnt effectors Tcf7, Tcf7l1 and Tcf7l2 was validated by qPCR (Fig. 3b). The up-regulation of Wnt3a and TCF7, and the down-regulation of Tcf7l1 and Tcf7l2 confirmed an over-activation of the Wnt pathway.

MiR-125a-3p over-expression in OPCs alters the expression of adhesion molecules and gap junctions

The list of differentially expressed genes after miR-125a-3p over-expression was also evaluated by means of a Gene Ontology-based analysis, which allows to identify common biological processes and functions for differentially expressed genes. The gene-ontology-based analysis showed that miR-125a-3p over-expression alters several biological processes related to oligodendrocyte maturation and myelination (Table 2). The most significant biological processes, "Role of cell-cell and ECM-cell interactions in oligodendrocyte differentiation and myelination" and "Cell adhesion - Gap junctions", were studied more in detail by means of specific PCR arrays (i.e., "Extracellular Matrix & Adhesion Molecules" and "Gap Junctions), that allowed to simultaneously profile the expression of 84 genes important for these processes (see Table S2-S3 for the full gene list, fold changes and p-values). In the "Extracellular Matrix & Adhesion Molecules" array, after miR-125a-3p over-expression, statistically significant expression changes were detected in 23 out of 84 genes (Fig. 4a-b). The 7 down-regulated genes were: Catna1, Cdh2, Col2a1, Mmp2, Tgfbi, Syt1 and Timp3. The 16 up-regulated genes were: Cd44, Fn1, Entpd1, Fbln1, Hapln1, Itgad, Itgam, Mmp14, Ncam1, Sell, Sparc, Spp1, Timp1, Timp2, Thbs2, and Lamb2. In the "Gap Junctions" array, after miR-125a-3p over-expression, statistical significance expression changes were detected in 19 of 84 genes (Fig. 5a-b). The 13 down-regulated genes were: Lpar1,

See published version at: https://doi.org/10.1007/s10571-020-00836-z

Cx32, Cx36, Grb2, Itpr2, Mapk3, Nras, Prkacb, Raf1, Sos2, Tjp2, Tubb4a, Tubb2b. The 6 up-regulated gene were: Cx43, Gucy1a2, Gucy1b3, Ma2k2, Map3k2, Tubg1. Globally, these results suggest that over-expression of miR-125a-3p alters the expression of several genes associated to cell-ECM and cell-cell communication, likely contributing to impair oligodendrocyte maturation and myelination.

Discussion

The identification of miRNA targets is an important means to elucidate their mode of action and eventually to develop new miRNA-based drugs (Marangon et al. 2019). However, it is worth mentioning that the action of a miRNA on a single specific gene transcript can be rather modest and totally insufficient to explain its pleiotropic biological effects. MiRNAs can indeed target hundreds of transcripts serially, simultaneously, and in concert with other transcriptional and epigenetic factors acting on the same pathways. On one hand, this is the reason why a single miRNA can lead to a very powerful effect on cell survival, proliferation and differentiation (Ebert and Sharp 2012). On the other hand, due to this very peculiar mode of action, when studying miRNAs, it is necessary to adopt a global comprehensive approach focusing on entire biological pathways rather than single direct targets.

Several transcripts involved in pathways connected to myelination have been so far identified as direct targets of miR-125a-3p, such as Fyn-kinase (Ninio-Many et al. 2013), which plays a key role in regulating oligodendrocyte myelination during development (Peckham et al. 2016) and NRG1 (Yin et al. 2015), a potent chemoattractant that selectively regulates OPC migration and the extent of myelination during early CNS development (Ortega et al. 2012). In a previous study, we demonstrated that the inhibitory effect of miR-125a-3p on oligodendrocyte maturation in terms of expression of myelinating genes was significantly higher than the effect of the same miRNA on its already validated direct targets, including Fyn and Nrg1 (Lecca et al. 2016), suggesting an effect on multiple signaling cascades leading to terminal maturation. For this reason, the aim of the present study was to elucidate the mechanisms regulated by miR-125a-3p during OPC maturation by focusing on entire biological pathways rather than single direct targets. To this purpose, we performed a transcriptomic analysis after its over-expression and then we analyzed differentially expressed genes by means of two complementary approaches to identify common pathways and biological processes (Marangon 2018).
A first pathway-based analysis suggested that the expression changes of several genes in our dataset may be related to TCF7L2 signaling inactivation. TCF7L2 is an important effector of the Wnt/β-catenin pathway, that, as recently shown, can also act in a Wnt-independent manner by interacting with other co-factors (i.e. Kaiso and Sox10), to promote oligodendrocyte maturation (Zhao et al. 2016). Since it is widely known that constitutive activation of Wnt/β-catenin inhibits oligodendrocyte maturation (Hammond et al. 2015), we hypothesize that miR-125a-3p over-expression induces an over-activation of the Wnt pathway, which, in turn, prevents TCF7L2-mediated pro-myelinating effects. Our qPCR data on Wnt signaling after miR-125a-3p over-expression in OPCs revealed an up-regulation of the Wnt ligand Wnt3a, in parallel to up-regulation of Tcf7 and down-regulation of Tcf7l1 and Tcf7l2 downstream effectors, expression changes that have been previously associated to Wnt-signaling over-stimulation (Kuwahara et al. 2014), in line with our hypothesis.

See published version at: https://doi.org/10.1007/s10571-020-00836-z

A second ontology-based approach allowed us to identify common biological processes for differentially expressed genes, revealing that miR-125a-3p can modulate several processes related to oligodendrocyte maturation and myelination, such as "adhesion molecules and ECM proteins", "gap junctions" and "thyroid hormone signaling". The PCR arrays "Extracellular Matrix & Adhesion Molecules" and "Gap Junctions" were used to simultaneously profile the expression of 84 genes involved in these processes. Our data show that miR-125a-3p over-expression in OPCs alters the expression of several classes of ECM, adhesion molecules, such as catenin (Catn), collagens (Col), integrins (Itg), laminins (Lam) and metalloproteinases (Mmp). Despite some of these classes of molecules may have a dispensable role during OPC *in vitro* maturation, several reports in literature show that such alterations are usually associated to dysmyelinating conditions, suggesting that our data could have a high relevance *in vivo*. For example, it has been reported that disruption of integrin-ECM connection leads to aberrant process and myelin sheath formation (Olsen and Ffrench-Constant 2005). Moreover, antibodies blocking β1-integrin reduce the ability of OPCs to extend their processes *in vitro* (Buttery and ffrench-Constant 1999). Interestingly, one of the downstream mechanisms that mediate integrin effects on OPC morphological differentiation is the activation of the Fyn kinase, which, in turn, regulates several downstream signaling, such as Rac1 and RhoA (O'Meara et al. 2011), suggesting that, also in this case, miR-125a-3p can influence several actors involved in a common pathway. Other reports have shown that β1-integrin can also form a functional signaling unit by associating to contactin 1 (Cntn1) and regulate Fyn activation by controlling its phosphorylation state (Laursen et al. 2009). These data suggest that miR-125a-3p over-expression not only directly influences Fyn expression, but can also indirectly control its activity by modulating upstream signaling molecules.

The "ECM & Adhesion Molecules" expression profile highlighted an up-regulation of genes that are typically expressed by other glial cells, such as CD44 and Spp1, which have been reported to be induced also in oligodendrocytes following various insults to the nervous system, including demyelinating conditions (Tuohy et al. 2004). Interestingly, the oligodendroglial over-expression of CD44, a transmembrane glycoprotein expressed by astrocytes and microglia in the CNS, causes a strong reduction in the number of myelinated fibers, leading to a dysmyelinating phenotype (Tuohy et al. 2004). Moreover, a recent study demonstrated that CD44 is a positive regulator of canonical Wnt signaling (Schmitt et al. 2015). The gene Spp1 encodes for Osteopontin (OPN), a secreted glycoprotein with cytokine-like, chemotactic and anti-apoptotic properties that activates CD44 itself (Selvaraju et al. 2004). In EAE, the administration of recombinant OPN induces relapses, whereas treatment with anti-OPN antibodies ameliorates the disease (Hur et al. 2007). Several studies have demonstrated that MS patients present a strong increase of OPN levels in CSF and blood, in particular in the active phase (Agah et al. 2018). Moreover, in patients with active MS, who underwent disease-modifying treatments, the levels of anti-OPN antibodies were higher than in untreated patients and were associated with low MS severity score (Clemente et al. 2017).

Furthermore, down-regulation of the tissue inhibitor of metalloproteinases Timp3, as well as up-regulation of Mmp14, Col1a1, Col3a1, Fn1, Lamb2 and Thbs2 were instead found in human MS active lesions (Haddock et al. 2006; Mohan et al. 2010), suggesting that miR-125a-3p over-expression can recapitulate some typical

pathological features that OPCs acquire in demyelinating environment. In line with this hypothesis, we have previously found up-regulated levels of miR-125a-3p in the CSF of MS patients in relapsing phase (Lecca et al. 2016).

We have also shown that the over-expression of miR-125a-3p alters genes encoding components, interactors, and regulators of GJs, such as pannexin 2 (Panx2), connexins (Cx29, Cx32, Cx43), tubulins (Tubb4a, Tubb2b), surface receptors (Lpar1, Egfr) and protein kinase (Pkc, Nras, Raf1, Map2k2, Map3k2, Mapk3). In the CNS, glial cells express different sets of connexins, which, by forming heterodimers, allow the direct passage of ions and small molecules between different cell types (i.e. oligodendrocyte-to-astrocyte coupling, O-A). Oligodendrocytes mainly express Cx47, Cx32 and Cx29, that may also participate to the formation of oligodendrocyte-to-oligodendrocyte (O-O) gap junctional coupling (Wasseff and Scherer 2011). The GJs expression profile highlighted a global alteration in mitogen-activated protein kinase (MAPK) pathway, as suggested by the change in the expression of Nras, Raf1, MEK2 (Map2k2), MEKK2 (Map3k2) and ERK-1 (Mapk3). Interestingly, it has been previously established that Cx subcellular trafficking, GJ gating, function and turnover are phosphorylation-dependent and that the mechanism involves the recruitment of MAPK family members (Chen et al. 2013).

We also observed a strong down-regulation of LPAR1 (lysophosphatidic acid receptor 1), a G-protein coupled receptor known to modulate the formation of processes in differentiating oligodendrocytes, allowing their terminal maturation (Garcia-Diaz et al. 2015). Mice lacking the LPA1 receptor exhibit a reduction in cortical oligodendrocytes and defective quantity, quality, and organization of myelinated fibers (Garcia-Diaz et al. 2015). Interestingly, LPA1 receptor stimulation activates MAPK pathway in oligodendrocytes by coupling to Gq subunits and activating PLC and PKC pathways (Yu et al. 2004). Our data show that miR-125a-3p indeed acts at different levels of the GJs signaling, by simultaneously affecting the expression of several key players in the pathway, such as surface receptors (Lpar1), intracellular kinases (MAPKs, PKC) and connexins (Cx47, Cx32 and Cx29).

Of note, the importance of oligodendroglial GJs in myelin formation and maintenance is also demonstrated by the finding that their genetic mutation is related to human disorders characterized by a dysmyelinating phenotype (Papaneophytou et al. 2018). In line with these observations, we hypothesize that the alteration in the expression levels of GJ genes observed after miR-125a-3p over-expression may prevent oligodendrocytes from reaching the myelinating state. Considering that miRNAs do not necessarily lead to the degradation of target mRNAs, a future proteomic analysis after miR-125a-3p over-expression will help to interpret and strengthen these transcriptomic data.

In conclusion, these data suggest that miR-125a-3p modulates different aspects of OPC development, playing an essential role in cell differentiation, myelination and dysmyelination. The identification of the pathways altered by miR-125a-3p will allow not only to define the networks orchestrating these mechanisms, but also to unveil new pharmacological targets to foster re-myelination in diseases characterized by myelination defects.

See published version at: https://doi.org/10.1007/s10571-020-00836-z

Methods

OPC isolation and transfection

Primary oligodendrocyte precursor cells were obtained from postnatal day 2 Sprague-Dawley rat cerebral cortices (Chen et al. 2007). Cortical tissues were incubated with 10 ml trypsin-EDTA solution containing 1% DNAse I (final concentration 0.01 mg/ml) (Sigma-Aldrich) for 30 minutes in a water bath at 37°C for tissue disaggregation. After the incubation, trypsin was inactivated with HBSS containing 10% of fetal bovine serum (FBS, Euroclone) and tissues were further triturated mechanically with a Pasteur pipet. The cellular suspension was passed through a 100 μm cell strainer (BD) in order to eliminate undissociated tissue residues. Cells were plated in T75 poly-D-lysine (final concentration 10 μg/ml, Sigma-Aldrich) coated flasks in DMEM high glucose (Euroclone), 2 mM L-glutamine (Sigma-Aldrich), 1 mM Sodium pyruvate (Sigma-Aldrich), Penicillin 100 U/ml-Streptomycin 100 μg/ml (Euroclone), 2.5 μg/ml Fungizone (Euroclone) and 20% FBS.

After 8 days in culture, flasks were shaken for 3-4 hours to promote OPC detaching. The OPC cell suspension was then transferred into a 50 ml tube, centrifuged at 1200 rpm for 15 minutes and resuspended in a small amount of Neurobasal (Life Technologies) containing 2 mM L-Glutamine, 1% of Penicillin 100 U/ml-Streptomycin 100 μg/ml and 2% of B27 (Life Technologies). OPCs were plated onto poly-D,L-ornithine-coated (final concentration 50 μg/ml; Sigma-Aldrich) 6-cm dishes (1.5 x 10^5 cells) for PCR array and qRT-PCR experiments. Cells were plated in Neurobasal medium supplemented with 2% B27 (Life Technologies), 2 mM L-glutamine, 10 ng/ml human platelet-derived growth factor BB (Sigma-Aldrich), and 10 ng/ml human basic fibroblast growth factor (Life Technologies) to promote proliferation for 3 days. OPCs were transfected immediately after switching from proliferating to differentiating medium (in the presence of the T3 hormone). MiR-125a-3p mimic (Dharmacon) was transfected at the final concentration of 50 nM with Lipofectamine RNAiMAX reagent (Life Technologies) following the manufacturer's protocol. A scrambled miRNA transfection was included as negative control. Cells were lysed with RLT buffer (Qiagen) 48 hours after transfection. For each independent experiment four postnatal day 2 rats were sacrificed to obtain the necessary number of OPCs.

Microarray

Total RNA was extracted by means of RNeasy Micro kit (Qiagen) following the manufacturer's protocol. RNA quality was assessed with Agilent 2100 Bioanalyzer (Agilent Technologies). RNA with RNA integrity number (RIN) > 7 was used for microarray analysis. Labeled cRNA was synthesized from 100 ng of total RNA using the Low Input Quick-Amp Labeling Kit, one color (Agilent Technologies) in the presence of cyanine 3-CTP. The microarray hybridization was performed by the Microarray Facility, Laboratorio per le Tecnologie delle Terapie Avanzate (LTTA), Ferrara, Italy. Total RNA was hybridized on SurePrint G3 Rat Gene Expression Microarrays (#G4858A-074036, Agilent Technologies). This microarray consists of 60-mer DNA probes synthesized in situ, which represent 30,584 rat transcripts. Hybridization was performed at 65°C for 17

hours in a rotating oven. One-color gene expression analysis was performed according to manufacturer's procedure. Feature Extraction 10.7.3 software (Agilent Technologies) was used to obtain microarray raw-data. A fold change of ±1.5 and a FDR-adjusted p-value < 0.05 were considered to obtain the list of genes differentially expressed between the two experimental conditions. Datasets and raw data are publicly-available in GEO Profile (GEO ID: 200143876).

Bioinformatic analysis

QIAGEN's Ingenuity® Pathway Analysis (IPA®, QIAGEN Redwood City, www.qiagen.com/ingenuity) was used to perform the upstream regulator analysis on differentially expressed genes after miR-125a-3p over-expression. Z score > 2 indicates that the signaling guided by a transcriptional regulator is likely activated, whereas Z score < 2 indicates that it is likely inhibited in the experimental condition.

The software Metacore™ was used to perform an ontology-based clusterization on differentially expressed genes after miR-125a-3p over-expression in OPCs, to identify common biological processes.

Pathway-focused PCR arrays.

Total RNA was extracted by means of RNeasy Micro kit (Qiagen) following the manufacturer's protocol. The PCR arrays "Wnt signaling targets" (PARN-243ZD), "Extracellular Matrix & Adhesion Molecules" (PARN-013ZD) and "Gap Junction" (PARN-144Z) were used to identify genes differentially expressed in OPCs after miR-125a-3p over-expression compared to negative control (See Supplementary material for the full gene list). For each PCR array, cDNA synthesis was performed starting from 500 ng of DNase pre-treated total RNA using RT2 First Strand Kit (Qiagen), following manufacturer's protocol. RT2 Profiler PCR Array (SABiosciences) and RT2 SYBRgreen Mastermix (Qiagen) were used to measure gene expression levels. Each array includes five housekeeping genes, that enable normalization of data, a genomic DNA control, that specifically detects genomic DNA contamination, a reverse transcription control, that tests the efficacy of the reverse-transcription reaction and a positive PCR control, that tests the efficacy of the polymerase chain reaction itself. Data were analysed by RT2 Profiler PCR Array data analysis center v. 3.5 (Qiagen).

Total RNA extraction, retrotranscription and qPCR analysis

Total RNA was extracted by using RNeasy plus micro kit (Qiagen) by following the manufacturer's protocol. For gene expression analysis, cDNA synthesis was performed starting from 400ng of total RNA using SensiFAST™ cDNA synthesis kit (Bioline). The expression of Sox2, Wnt3a, Tcf7, Tcf7l1 and Tcf7l2 was assessed by means of pre-validated PrimePCR assay (Biorad) and SensiFAST™ SYBR Supermix (Bioline). using CFX96 real time PCR system (Biorad) following the manufacturer's protocol. Relative gene expression was calculated by the ΔCt method normalizing to GAPDH expression.

Statistical analysis

Data are presented as Log2(fold change) mean ±SEM and were analysed with the GraphPad Prism 7.04 software. Shapiro-Wilk normality test was performed to assess normal distribution of data. One sample two

tailed t-test was performed to assess data statistical significance. $P < 0.05$ was considered as statistically significant. Data with $0.05 < \text{p-value} < 0.1$ were indicated with § symbol.

References

Agah E, Zardoui A, Saghazadeh A, Ahmadi M, Tafakhori A, Rezaei N (2018) Osteopontin (OPN) as a CSF and blood biomarker for multiple sclerosis: A systematic review and meta-analysis PloS one 13:e0190252 doi:10.1371/journal.pone.0190252

Buttery PC, ffrench-Constant C (1999) Laminin-2/integrin interactions enhance myelin membrane formation by oligodendrocytes Molecular and cellular neurosciences 14:199-212 doi:10.1006/mcne.1999.0781

Chen VC, Gouw JW, Naus CC, Foster LJ (2013) Connexin multi-site phosphorylation: mass spectrometry-based proteomics fills the gap Biochimica et biophysica acta 1828:23-34 doi:10.1016/j.bbamem.2012.02.028

Chen Y, Balasubramaniyan V, Peng J, Hurlock EC, Tallquist M, Li J, Lu QR (2007) Isolation and culture of rat and mouse oligodendrocyte precursor cells Nature protocols 2:1044-1051 doi:10.1038/nprot.2007.149

Clemente N et al. (2017) Role of Anti-Osteopontin Antibodies in Multiple Sclerosis and Experimental Autoimmune Encephalomyelitis Frontiers in immunology 8:321 doi:10.3389/fimmu.2017.00321

Ebert MS, Sharp PA (2012) Roles for microRNAs in conferring robustness to biological processes Cell 149:515-524 doi:10.1016/j.cell.2012.04.005

Garcia-Diaz B et al. (2015) Loss of lysophosphatidic acid receptor LPA1 alters oligodendrocyte differentiation and myelination in the mouse cerebral cortex Brain structure & function 220:3701-3720 doi:10.1007/s00429-014-0885-7

Gurtan AM, Sharp PA (2013) The role of miRNAs in regulating gene expression networks Journal of molecular biology 425:3582-3600 doi:10.1016/j.jmb.2013.03.007

Haddock G, Cross AK, Plumb J, Surr J, Buttle DJ, Bunning RA, Woodroofe MN (2006) Expression of ADAMTS-1, -4, -5 and TIMP-3 in normal and multiple sclerosis CNS white matter Multiple sclerosis 12:386-396 doi:10.1191/135248506ms1300oa

Hammond E et al. (2015) The Wnt effector transcription factor 7-like 2 positively regulates oligodendrocyte differentiation in a manner independent of Wnt/beta-catenin signaling The Journal of neuroscience : the official journal of the Society for Neuroscience 35:5007-5022 doi:10.1523/JNEUROSCI.4787-14.2015

Hur EM, Youssef S, Haws ME, Zhang SY, Sobel RA, Steinman L (2007) Osteopontin-induced relapse and progression of autoimmune brain disease through enhanced survival of activated T cells Nature immunology 8:74-83 doi:10.1038/ni1415

Kuwahara A, Sakai H, Xu Y, Itoh Y, Hirabayashi Y, Gotoh Y (2014) Tcf3 represses Wnt-beta-catenin signaling and maintains neural stem cell population during neocortical development PloS one 9:e94408 doi:10.1371/journal.pone.0094408

Laursen LS, Chan CW, ffrench-Constant C (2009) An integrin-contactin complex regulates CNS myelination by differential Fyn phosphorylation The Journal of neuroscience : the official journal of the Society for Neuroscience 29:9174-9185 doi:10.1523/JNEUROSCI.5942-08.2009

Lecca D et al. (2016) MiR-125a-3p timely inhibits oligodendroglial maturation and is pathologically up-regulated in human multiple sclerosis Scientific reports 6:34503 doi:10.1038/srep34503

Marangon D (2018) MicroRNA-125a-3p negatively regulates oligodendroglial maturation and re-myelination: molecular mechanisms and clinical implications. Dissertation, University of Milan

Marangon D, Raffaele S, Fumagalli M, Lecca D (2019) MicroRNAs change the games in central nervous system pharmacology Biochemical pharmacology 168:162-172 doi:10.1016/j.bcp.2019.06.019

Mohan H et al. (2010) Extracellular matrix in multiple sclerosis lesions: Fibrillar collagens, biglycan and decorin are upregulated and associated with infiltrating immune cells Brain pathology 20:966-975 doi:10.1111/j.1750-3639.2010.00399.x

Ninio-Many L, Grossman H, Shomron N, Chuderland D, Shalgi R (2013) microRNA-125a-3p reduces cell proliferation and migration by targeting Fyn Journal of cell science 126:2867-2876 doi:10.1242/jcs.123414

Nualart-Marti A, Solsona C, Fields RD (2013) Gap junction communication in myelinating glia Biochimica et biophysica acta 1828:69-78 doi:10.1016/j.bbamem.2012.01.024

O'Meara RW, Michalski JP, Kothary R (2011) Integrin signaling in oligodendrocytes and its importance in CNS myelination Journal of signal transduction 2011:354091 doi:10.1155/2011/354091

Olsen IM, Ffrench-Constant C (2005) Dynamic regulation of integrin activation by intracellular and extracellular signals controls oligodendrocyte morphology BMC biology 3:25 doi:10.1186/1741-7007-3-25

Ortega MC, Bribian A, Peregrin S, Gil MT, Marin O, de Castro F (2012) Neuregulin-1/ErbB4 signaling controls the migration of oligodendrocyte precursor cells during development Experimental neurology 235:610-620 doi:10.1016/j.expneurol.2012.03.015

Papaneophytou CP et al. (2018) Regulatory role of oligodendrocyte gap junctions in inflammatory demyelination Glia 66:2589-2603 doi:10.1002/glia.23513

Peckham H et al. (2016) Fyn is an intermediate kinase that BDNF utilizes to promote oligodendrocyte myelination Glia 64:255-269 doi:10.1002/glia.22927

Schmitt M, Metzger M, Gradl D, Davidson G, Orian-Rousseau V (2015) CD44 functions in Wnt signaling by regulating LRP6 localization and activation Cell death and differentiation 22:677-689 doi:10.1038/cdd.2014.156

Selvaraju R et al. (2004) Osteopontin is upregulated during in vivo demyelination and remyelination and enhances myelin formation in vitro Molecular and cellular neurosciences 25:707-721 doi:10.1016/j.mcn.2003.12.014

Tuohy TM et al. (2004) CD44 overexpression by oligodendrocytes: a novel mouse model of inflammation-independent demyelination and dysmyelination Glia 47:335-345 doi:10.1002/glia.20042

Wasseff SK, Scherer SS (2011) Cx32 and Cx47 mediate oligodendrocyte:astrocyte and oligodendrocyte:oligodendrocyte gap junction coupling Neurobiology of disease 42:506-513 doi:10.1016/j.nbd.2011.03.003

Yin F et al. (2015) MiR-125a-3p regulates glioma apoptosis and invasion by regulating Nrg1 PloS one 10:e0116759 doi:10.1371/journal.pone.0116759

Yu N, Lariosa-Willingham KD, Lin FF, Webb M, Rao TS (2004) Characterization of lysophosphatidic acid and sphingosine-1-phosphate-mediated signal transduction in rat cortical oligodendrocytes Glia 45:17-27 doi:10.1002/glia.10297

Zhao C et al. (2016) Dual regulatory switch through interactions of Tcf7l2/Tcf4 with stage-specific partners propels oligodendroglial maturation Nature communications 7:10883 doi:10.1038/ncomms10883

Figures

See published version at: https://doi.org/10.1007/s10571-020-00836-z

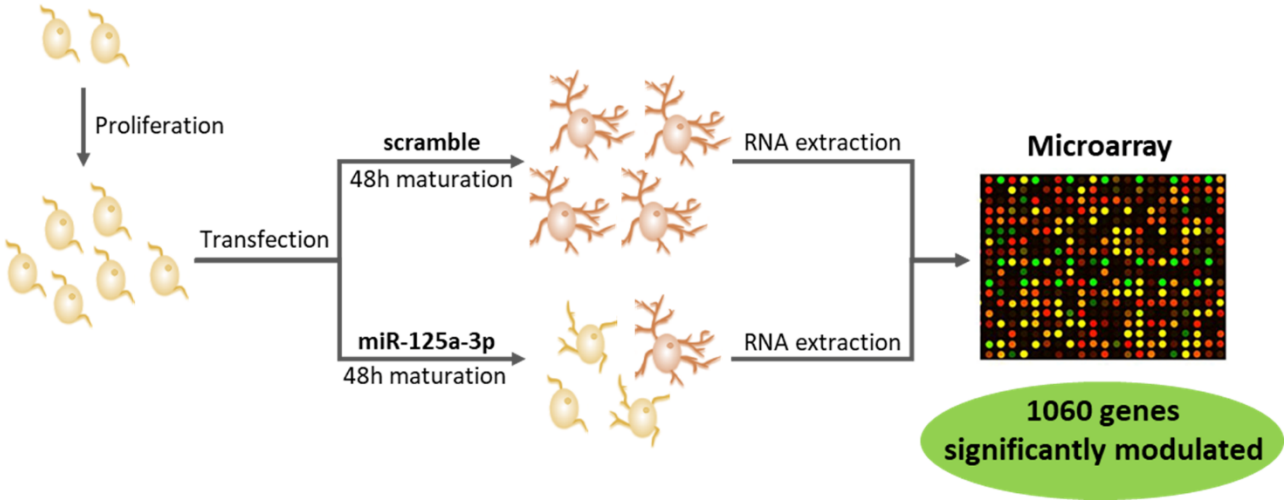

Fig.1 Gene expression profiling of OPCs after miR-125a-3p over-expression. Primary cultured OPCs were grown for three days in presence of growth factors, then they were transfected with the negative control or miR-125a-3p mimic in the presence of the T3 hormone to promote cell maturation and lysed 48 hours after transfection, for the subsequent RNA extraction and microarray analysis. The microarray revealed 1060 genes significantly modulated after miR-125a-3p over-expression

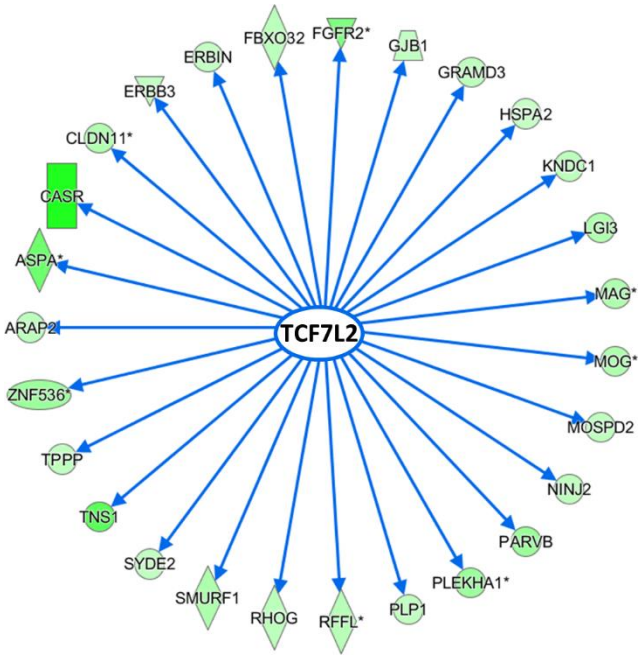

Fig. 2 MiR-125a-3p over-expression represses TCF7L2 signaling in OPCs. The scheme shows that the alteration of multiple genes after miR-125a-3p over-expression could be related to TCF7L2 signaling inhibition. Arrows represent negative interaction (leads to inhibition). All the transcripts were found down-regulated in the experimental dataset. Shape intensity directly correlate to the entity of the down-regulation.

See published version at: https://doi.org/10.1007/s10571-020-00836-z

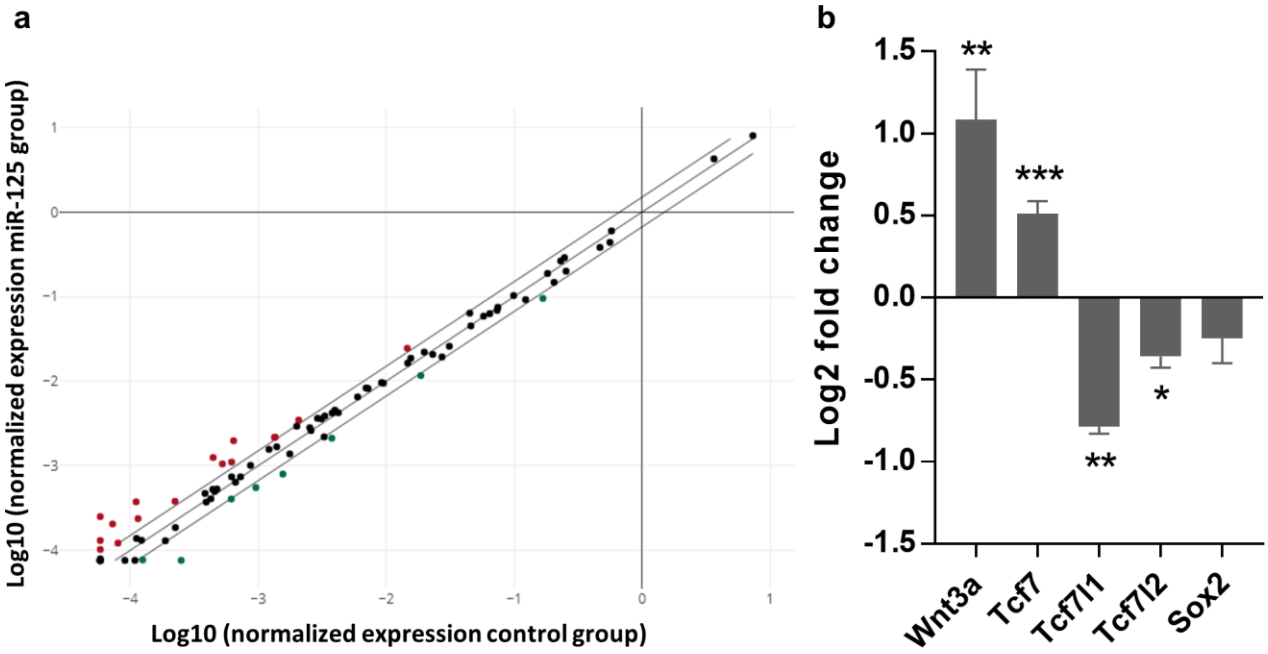

Fig. 3 Evaluation of the expression of Wnt targets after miR-125a-3p over-expression in OPCs. (a) Scatter plot comparing the normalized expression of each genes of the "Wnt targets" PCR array between the two groups (miR-125a-3p over-expression vs. negative control). Upper dots represent genes up-regulated, lower dots represent genes down-regulated. Black dots indicate unchanged genes. Cut-off = ±1.5 **(b)** Histogram shows Log2FC of Sox2, Wnt3a, Tcf7, Tcf7L1 and Tcf7L2 after mir-125a-3p over-expression in OPCs (control set to 0; n=5 for each group). One sample t-test; *p<0.05; **p<0.01; ***p<0.001.

See published version at: https://doi.org/10.1007/s10571-020-00836-z

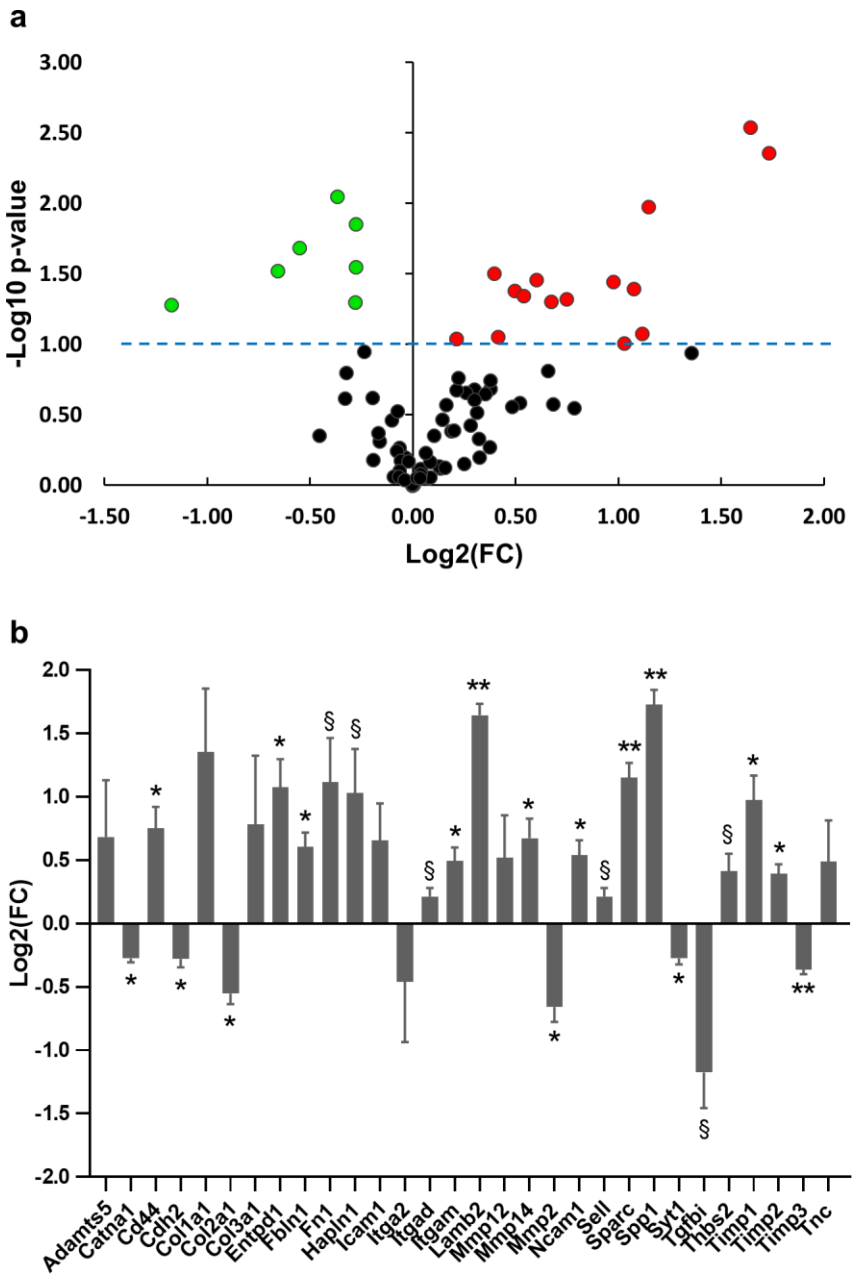

Fig. 4 Evaluation of the expression of Extracellular Matrix & Adhesion Molecules after miR-125a-3p over-expression in OPCs. (a) Volcano plot of the "Extracellular Matrix & Adhesion Molecules" PCR array. The relative fold change of each gene was calculated by comparing the expression in miR-125a-3p over-expressing and scramble RNA-treated OPCs (N=3 for each group). Log2(fold change) are plotted against -Log10(p-value). Green and red indicators show down-regulated and upregulated genes, respectively. The blue line indicates a p-value of 0.1. **(b)** Histogram shows Log2(FC) of selected adhesion molecules and ECM genes (control set to 0). One sample t-test; § $p<0.1$; *$p<0.05$; **$p<0.01$.

See published version at: https://doi.org/10.1007/s10571-020-00836-z

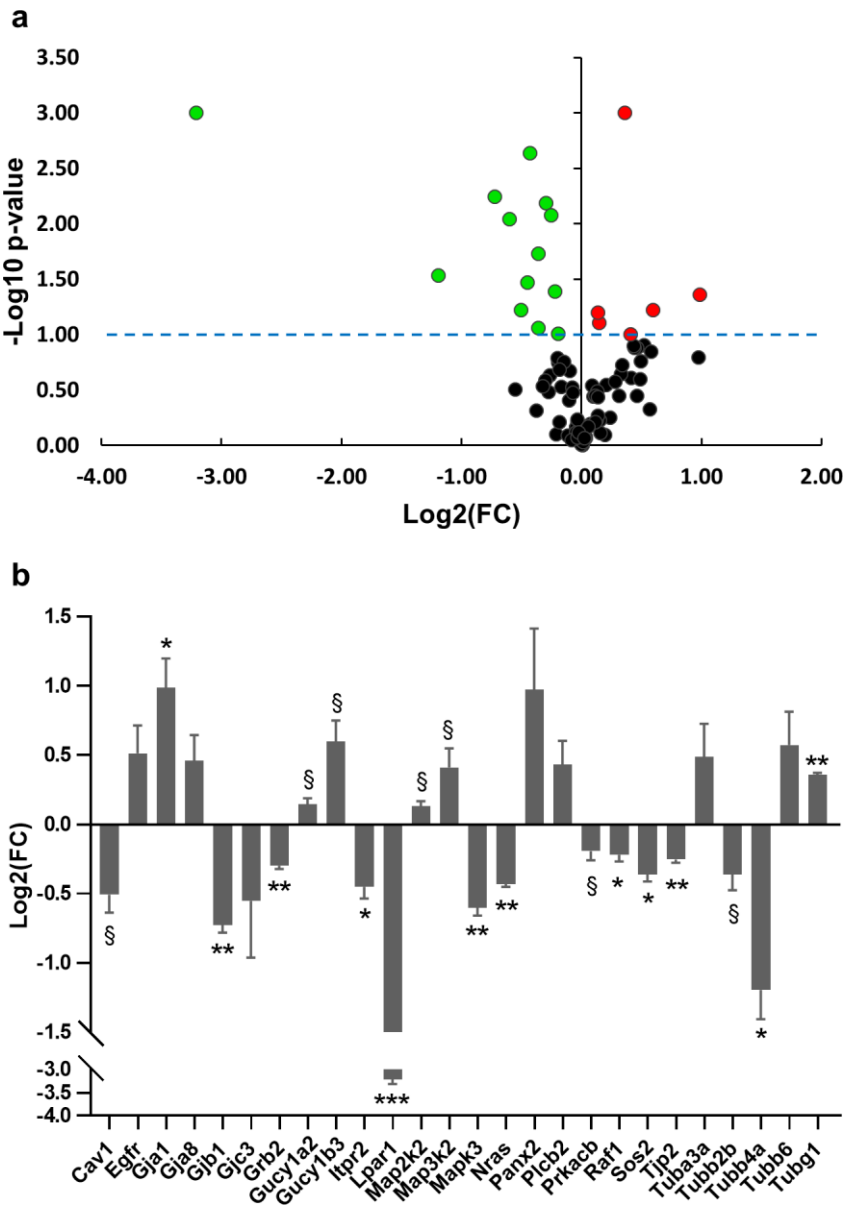

Fig. 5 Gap Junctions PCR array expression profile after miR-125a-3p over-expression in OPCs. (a) Volcano plot of the "Gap Junctions" PCR array. The relative fold change of each gene was calculated by comparing the expression in miR-125a-3p over-expressing and scramble RNA-treated OPCs (N=3 for each group). Log2(fold change) are plotted against -Log10(p-value). Green and red indicators show down-regulated and upregulated genes, respectively. The blue line indicates a p-value of 0.1. **(b)** Histogram shows Log2(FC) of selected components, interactors, and regulators of gap junction (control set to 0). One sample t-test; § $p<0.1$; *$p<0.05$; **$p<0.01$.

Table 1 Upstream regulator analysis. The over-expression of miR-125a-3p in OPCs caused a statistically significant change in the expression of 1060 transcripts. These differentially expressed genes were analyzed with the Ingenuity Pathway Analysis tool (IPA) performing an upstream regulator analysis, to identify possible alterations in the activity of gene expression master regulators, that may be responsible for the changes

See published version at: https://doi.org/10.1007/s10571-020-00836-z

observed in the experimental dataset. The table shows the most promising master regulators resulting from the analysis, with the relative p-value and number of targets modulated. Cut-off: Z= ±1

Master regulator	Molecule type	Prediction	Z Score	p-value	Number of targets
TCF7L2	**transcription factor**	**Inhibited**	**-5.186**	**5.21E-08**	**27**
BDNF	growth factor	Inhibited	-2.381	4.23E-06	26
CXCL8	cytokine	Inhibited	-1.219	8.54E-06	8
1L1B	cytokine	Activated	1.349	3.26E-05	30
IFNG	cytokine	Activated	2.541	1.26E-04	36
TGFB1	growth factor	Activated	1.451	1.69E-04	55
LIF	cytokine	Activated	1.362	3.29E-04	14
STAT1	transcription factor	Activated	2.592	3.95E-04	14
IL6R	receptor	Activated	2.236	6.06E-04	7
MKNK1	kinase	Activated	2.714	6.47E-04	11

Table 2. Ontology-based clusterization with Metacore. The software Metacore was used to perform an ontology-based analysis of the 1060 differentially expressed genes, in order to identify common biological processes and functions. In table are reported the resulting more significant biological processes and the relative associated genes from the experimental dataset. In bold, biological processes selected for subsequent studies

Biological Process	Total	FDR p-value	N°of targets	Targets in the dataset
Role of cell-cell and ECM-cell interactions in oligodendrocyte differentiation and myelination	34	9.1E-05	9	Claudin-11, PLP1, Connexin 43, Connexin 26, Reticulon 4, MAG, GJC3, Myelin basic protein, Connexin 32
Cell adhesion_Gap junctions	30	1.6E-02	6	PKC, Connexin 43, Connexin 31, Connexin 26, Connexin 32, Tubulin beta
Role of Thyroid hormone in regulation of oligodendrocyte differentiation	48	2.6E-02	7	TR-beta, PLP1, p73, MOG, MAG, Myelin basic protein, OATP-A
ATM / ATR regulation of G2 / M checkpoint	26	3.1E-02	5	Chk1, Chk2, Cyclin B, Claspin, GADD45 beta
Substance P-stimulated expression of proinflammatory cytokines via MAPKs	43	3.9E-02	6	PKC-delta, PLC-beta, Substance P extracellular region, CCL13, c-Jun, GRO-2
Oxidative stress_Activation of NADPH oxidase	59	3.9E-02	7	PKC, PKC-delta, p47-phox, PLC-beta, p22-phox, TRIO, Rac2
HDL-mediated reverse cholesterol transport	44	3.9E-02	6	Pre beta-1 HDL, Nascent HDL, Large apoE-rich HDL, APOA1, PLTP, APOE
Cytoskeleton remodeling	102	5.3E-02	9	Fibronectin, MyHC, MYLK1, MLCK, Collagen I, TGF-beta receptor type I, TRIO, c-Jun, LIMK2

See published version at: https://doi.org/10.1007/s10571-020-00836-z

Supplementary Table 1. RT² Profiler™ PCR Array Rat WNT Signaling Targets (PARN-243Z)

Symbol	Description	GeneBank	Fold Change
Abcb1a	ATP-binding cassette, sub-family B (MDR/TAP), member 1A	NM_133401	2.81
Ahr	Aryl hydrocarbon receptor	NM_013149	0.95
Angptl4	Angiopoietin-like 4	NM_199115	1.30
Antxr1	Anthrax toxin receptor 1	NM_001044249	0.99
Axin2	Axin 2	NM_024355	1.17
Bglap	Bone gamma-carboxyglutamate (gla) protein	NM_013414	1.09
Birc5	Baculoviral IAP repeat-containing 5	NM_022274	1.42
Bmp4	Bone morphogenetic protein 4	NM_012827	0.72
Btrc	Beta-transducin repeat containing	NM_001007148	1.04
Cacna2d3	Calcium channel, voltage-dependent, alpha2/delta subunit 3	NM_175595	1.19
Ccnd1	Cyclin D1	NM_171992	1.00
Ccnd2	Cyclin D2	NM_022267	1.20
Cd44	Cd44 molecule	NM_012924	1.30
Cdh1	Cadherin 1	NM_031334	1.70
Cdkn2a	Cyclin-dependent kinase inhibitor 2A	NM_031550	1.19
Cdon	Cdon homolog (mouse)	NM_017358	1.13
Cebpd	CCAAT/enhancer binding protein (C/EBP), delta	NM_013154	1.01
Ctgf	Connective tissue growth factor	NM_022266	1.60
Cubn	Cubilin (intrinsic factor-cobalamin receptor)	NM_053332	2.81
Dab2	Disabled homolog 2 (Drosophila)	NM_024159	1.19
Dkk1	Dickkopf homolog 1 (Xenopus laevis)	NM_001106350	0.82
Dlk1	Delta-like 1 homolog (Drosophila)	NM_053744	1.62
Dpp10	Dipeptidylpeptidase 10	NM_001012205	1.11
Efnb1	Ephrin B1	NM_017089	1.00
Egfr	Epidermal growth factor receptor	NM_031507	0.95
Egr1	Early growth response 1	NM_012551	1.67
Enpp2	Ectonucleotide pyrophosphatase/phosphodiesterase 2	NM_057104	0.81
Ets2	V-ets erythroblastosis virus E26 oncogene homolog 2	NM_001107107	1.09
Fgf20	Fibroblast growth factor 20	NM_023961	1.30
Fgf4	Fibroblast growth factor 4	NM_053809	1.30
Fgf7	Fibroblast growth factor 7	NM_022182	0.30
Fgf9	Fibroblast growth factor 9	NM_012952	1.29
Fn1	Fibronectin 1	NM_019143	3.08
Fosl1	Fos-like antigen 1	NM_012953	0.78
Fst	Follistatin	NM_012561	0.66
Gdf5	Growth differentiation factor 5	XM_001066344	1.30
Gdnf	Glial cell derived neurotrophic factor	NM_019139	1.30
Gja1	Gap junction protein, alpha 1	NM_012567	1.67
Id2	Inhibitor of DNA binding 2	NM_013060	1.14
Igf1	Insulin-like growth factor 1	NM_178866	2.06
Igf2	Insulin-like growth factor 2	NM_031511	1.20
Il6	Interleukin 6	NM_012589	1.23

See published version at: https://doi.org/10.1007/s10571-020-00836-z

Irs1	Insulin receptor substrate 1	NM_012969	0.98
Jag1	Jagged 1	NM_019147	0.83
Klf5	Kruppel-like factor 5	NM_053394	1.78
Lef1	Lymphoid enhancer binding factor 1	NM_130429	1.16
Lrp1	Low density lipoprotein-related protein 1	NM_001130490	0.71
Met	Met proto-oncogene	NM_031517	0.58
Mmp2	Matrix metallopeptidase 2	NM_031054	0.56
Mmp7	Matrix metallopeptidase 7	NM_012864	0.70
Mmp9	Matrix metallopeptidase 9	NM_031055	1.22
Myc	Myelocytomatosis oncogene	NM_012603	1.04
Nanog	Nanog homeobox	NM_001100781	1.11
Nrcam	Neuronal cell adhesion molecule	NM_013150	1.14
Nrp1	Neuropilin 1	NM_145098	0.51
Ntrk2	Neurotrophic tyrosine kinase, receptor, type 2	NM_012731	1.03
Pdgfra	Platelet derived growth factor receptor, alpha	NM_012802	0.79
Pitx2	Paired-like homeodomain 2	NM_019334	1.02
Plaur	Plasminogen activator, urokinase receptor	NM_017350	0.62
Pou5f1	POU class 5 homeobox 1	NM_001009178	1.36
Ppap2b	Phosphatidic acid phosphatase type 2B	NM_138905	0.97
Ppard	Peroxisome proliferator-activated receptor delta	NM_013141	1.11
Ptch1	Patched homolog 1 (Drosophila)	NM_053566	0.90
Ptgs2	Prostaglandin-endoperoxide synthase 2	NM_017232	2.24
Runx2	Runt-related transcription factor 2	NM_053470	0.69
Sfrp2	Secreted frizzled-related protein 2	NM_001100700	1.11
Six1	SIX homeobox 1	NM_053759	1.07
Smo	Smoothened homolog (Drosophila)	NM_012807	1.47
Sox2	SRY (sex determining region Y)-box 2	NM_001109181	0.57
Sox9	SRY-box containing gene 9	XM_001081628	1.25
T	T, brachyury homolog (mouse)	NM_001106209	0.96
Tcf7l1	Transcription factor 3	NM_001107865	0.63
Tcf4	Transcription factor 4	NM_053369	1.17
Tcf7	Transcription factor 7 (T-cell specific, HMG-box)	XM_006220666	3.37
Tcf7l2	Transcription factor 7-like 2 (T-cell specific, HMG-box)	NM_001191052	0.75
Tgfb3	Transforming growth factor, beta 3	NM_013174	1.11
Tle1	Transducin-like enhancer of split 1 (E(sp1) homolog, Drosophila)	NM_001173433	0.67
Twist1	Twist homolog 1 (Drosophila)	NM_053530	4.29
Vegfa	Vascular endothelial growth factor A	NM_031836	1.02
Wisp1	WNT1 inducible signaling pathway protein 1	NM_031716	1.52
Wisp2	WNT1 inducible signaling pathway protein 2	NM_031590	1.76
Wnt3a	Wingless-type MMTV integration site family, member 3A	NM_001107005	2.00
Wnt5a	Wingless-type MMTV integration site family, member 5A	NM_022631	1.15
Wnt9a	Wingless-type MMTV integration site family, member 9A	NM_001105783	0.84

See published version at: https://doi.org/10.1007/s10571-020-00836-z

Supplementary Table 2. RT² Profiler™ PCR Array Rat Extracellular Matrix & Adhesion Molecules (PARN-013Z).

Symbol	Description	GeneBank	Fold Change	p-value
Adamts1	ADAM metallopeptidase with thrombospondin type 1 motif, 1	NM_024400	0.87	0.239
Adamts2	ADAM metallopeptidase with thrombospondin type 1 motif, 2	NM_001137622	0.87	0.656
Adamts5	ADAM metallopeptidase with thrombospondin type 1 motif, 5	NM_198761	1.61	0.264
Adamts8	ADAM metallopeptidase with thrombospondin type 1 motif, 8	NM_001106811	1.30	0.206
Catna1	Catenin (cadherin associated protein), alpha 1	NM_001007145	0.83	0.014
Cd44	Cd44 molecule	NM_012924	1.68	0.048
Cdh1	Cadherin 1	NM_031334	1.00	0.992
Cdh2	Cadherin 2	NM_031333	0.82	0.051
Cdh3	Cadherin 3	NM_053938	0.97	0.635
Cdh4	Cadherin 4	XM_001061943	0.80	0.159
Cntn1	Contactin 1	NM_057118	0.80	0.240
Col1a1	Collagen, type I, alpha 1	NM_053304	2.56	0.115
Col2a1	Collagen, type II, alpha 1	NM_012929	0.68	0.021
Col3a1	Collagen, type III, alpha 1	NM_032085	1.72	0.282
Col4a1	Collagen, type IV, alpha 1	NM_001135009	0.95	0.542
Col4a2	Collagen, type IV, alpha 2	XM_001076134	1.23	0.209
Col4a3	Collagen, type IV, alpha 3	NM_001135759	0.95	0.566
Col5a1	Collagen, type V, alpha 1	NM_134452	0.96	0.668
Col6a1	Collagen, type VI, alpha 1	XM_215375	1.25	0.635
Col8a1	Collagen, type VIII, alpha 1	NM_001107100	1.30	0.179
Ctgf	Connective tissue growth factor	NM_022266	1.20	0.219
Ctnna2	Catenin (cadherin associated protein), alpha 2	NM_001106598	0.98	0.670
Ctnnb1	Catenin (cadherin associated protein), beta 1	NM_053357	1.02	0.857
Ecm1	Extracellular matrix protein 1	NM_053882	1.10	0.757
Emilin1	Elastin microfibril interfacer 1	NM_001106710	1.00	1.000
Entpd1	Ectonucleoside triphosphate diphosphohydrolase 1	NM_022587	2.11	0.040
Fbln1	Fibulin 1	NM_001127547	1.52	0.035
Fn1	Fibronectin 1	NM_019143	2.17	0.085
Hapln1	Hyaluronan and proteoglycan link protein 1	NM_019189	2.04	0.099
Icam1	Intercellular adhesion molecule 1	NM_012967	1.58	0.154
Itga2	Integrin, alpha 2	XM_345156	0.73	0.442
Itga3	Integrin, alpha 3	NM_001108292	0.89	0.484
Itga4	Integrin, alpha 4	NM_001107737	1.09	0.735
Itga5	Integrin, alpha 5 (fibronectin receptor, alpha polypeptide)	NM_001108118	0.95	0.790
Itgad	Integrin, alpha D	NM_031691	1.16	0.091
Itgae	Integrin, alpha E	NM_031768	1.21	0.375
Itgal	Integrin, alpha L	NM_001033998	1.24	0.302
Itgam	Integrin, alpha M	NM_012711	1.41	0.042
Itgav	Integrin, alpha V	NM_001106549	0.93	0.344
Itgb1	Integrin, beta 1	NM_017022	0.95	0.299
Itgb2	Integrin, beta 2	NM_001037780	1.05	0.892

See published version at: https://doi.org/10.1007/s10571-020-00836-z

Itgb3	Integrin, beta 3	NM_153720	1.03	0.767
Itgb4	Integrin, beta 4	NM_013180	1.03	0.884
Lama1	Laminin, alpha 1	NM_001108237	0.94	0.866
Lama2	Laminin, alpha 2	XM_008758643	1.03	0.889
Lama3	Laminin, alpha 3	XM_003753026	1.10	0.341
Lamb2	Laminin, beta 2	NM_012974	3.13	0.003
Lamb3	Laminin, beta 3	NM_001100841	1.06	0.874
Lamc1	Laminin, gamma 1	NM_053966	1.00	0.976
Mmp1	Matrix metallopeptidase 1a (interstitial collagenase)	NM_001134530	0.95	0.828
Mmp10	Matrix metallopeptidase 10	NM_133514	1.03	0.683
Mmp11	Matrix metallopeptidase 11	NM_012980	1.06	0.260
Mmp12	Matrix metallopeptidase 12	NM_053963	1.44	0.588
Mmp13	Matrix metallopeptidase 13	NM_133530	1.04	0.050
Mmp14	Matrix metallopeptidase 14 (membrane-inserted)	NM_031056	1.59	0.426
Mmp15	Matrix metallopeptidase 15	NM_001106168	0.89	0.441
Mmp16	Matrix metallopeptidase 16	NM_080776	1.07	0.866
Mmp2	Matrix metallopeptidase 2	NM_031054	0.63	0.030
Mmp3	Matrix metallopeptidase 3	NM_133523	1.29	0.534
Mmp7	Matrix metallopeptidase 7	NM_012864	1.16	0.211
Mmp8	Matrix metallopeptidase 8	NM_022221	1.28	0.224
Mmp9	Matrix metallopeptidase 9	NM_031055	1.14	0.413
Ncam1	Neural cell adhesion molecule 1	NM_031521	1.45	0.046
Ncam2	Neural cell adhesion molecule 2	NM_203409	1.12	0.267
Pecam1	Platelet/endothelial cell adhesion molecule 1	NM_031591	1.23	0.247
Postn	Periostin, osteoblast specific factor	NM_001108550	1.25	0.467
Sele	Selectin E	NM_138879	1.17	0.173
Sell	Selectin L	NM_019177	1.16	0.091
Selp	Selectin P	NM_013114	0.97	0.911
Sgce	Sarcoglycan, epsilon	NM_001002023	1.01	0.886
Sparc	Secreted protein, acidic, cysteine-rich (osteonectin)	NM_012656	2.21	0.011
Spock1	Sparc/osteonectin, (testican) 1	NM_001271297	1.02	0.885
Spp1	Secreted phosphoprotein 1	NM_012881	3.32	0.004
Syt1	Synaptotagmin I	NM_001033680	0.83	0.028
Tgfbi	Transforming growth factor, beta induced	NM_053802	0.44	0.053
Thbs1	Thrombospondin 1	NM_001013062	1.19	0.698
Thbs2	Thrombospondin 2	NM_001169138	1.33	0.089
Timp1	TIMP metallopeptidase inhibitor 1	NM_053819	1.97	0.036
Timp2	TIMP metallopeptidase inhibitor 2	NM_021989	1.32	0.032
Timp3	TIMP metallopeptidase inhibitor 3	NM_012886	0.78	0.009
Tnc	Tenascin C	NM_053861	1.40	0.276
Vcam1	Vascular cell adhesion molecule 1	NM_012889	1.15	0.409
Vcan	Versican	NM_001170558	0.85	0.112
Vtn	Vitronectin	NM_019156	1.11	0.749

See published version at: https://doi.org/10.1007/s10571-020-00836-z

Supplementary Table 3. RT² Profiler™ PCR Array Gap Junction (PARN-144Z)

Symbol	Description	GeneBank	Fold Change	p-value
Adcy1	Adenylate cyclase 1 (brain)	NM_001107239	0.86	0.788
Adcy2	Adenylate cyclase 2 (brain)	NM_031007	1.05	0.632
Adcy3	Adenylate cyclase 3	NM_130779	0.89	0.295
Adcy4	Adenylate cyclase 4	NM_019285	1.18	0.559
Adrb2	Adrenergic, beta-2-, receptor, surface	NM_012492	1.33	0.244
Cav1	Caveolin 1, caveolae protein	NM_031556	0.70	0.060
Cdk1	Cyclin-dependent kinase 1	NM_019296	1.15	0.283
Csnk1d	Casein kinase 1, delta	NM_139060	0.93	0.211
Ctnnb1	Catenin (cadherin associated protein), beta 1	NM_053357	0.97	0.621
Dbn1	Drebrin 1	NM_031024	1.02	0.819
Egfr	Epidermal growth factor receptor	NM_031507	1.43	0.124
Gja1	Gap junction protein, alpha 1	NM_012567	1.98	0.044
Gja10	Gap junction protein, alpha 10	NM_001173508	0.77	0.483
Gja3	Gap junction protein, alpha 3	NM_024376	0.92	0.812
Gja4	Gap junction protein, alpha 4	NM_021654	1.00	0.987
Gja5	Gap junction protein, alpha 5	NM_019280	1.11	0.586
Gja6	Gap junction protein, alpha 6	NM_019308	1.07	0.361
Gja8	Gap junction membrane channel protein alpha 8	NM_153465	1.37	0.131
Gjb1	Gap junction protein, beta 1	NM_017251	0.61	0.006
Gjb2	Gap junction protein, beta 2	NM_001004099	1.02	0.851
Gjb3	Gap junction protein, beta 3	NM_019240	0.97	0.684
Gjb4	Gap junction protein, beta 4	NM_053984	0.97	0.684
Gjb5	Gap junction protein, beta 5	NM_019241	1.06	0.286
Gjb6	Gap junction protein, beta 6	NM_053388	1.25	0.226
Gjc2	Gap junction protein, gamma 2	NM_001100784	0.88	0.615
Gjc3	Gap junction protein, gamma 3	XM_221997	0.68	0.308
Gjd2	Gap junction protein, delta 2	NM_019281	1.09	0.585
Gnai1	Guanine nucleotide binding protein, alpha inhibiting 1	NM_013145	0.95	0.300
Grb2	Growth factor receptor bound protein 2	NM_030846	0.82	0.007
Grm1	Glutamate receptor, metabotropic 1	NM_017011	1.00	0.970
Gucy1a2	Guanylate cyclase 1, soluble, alpha 2	NM_023956	1.11	0.079
Gucy1a3	Guanylate cyclase 1, soluble, alpha 3	NM_017090	1.10	0.537
Gucy1b3	Guanylate cyclase 1, soluble, beta 3	NM_012769	1.51	0.060
Hras	Harvey rat sarcoma virus oncogene	NM_001098241	0.99	0.893
Htr2a	5-hydroxytryptamine (serotonin) receptor 2A	NM_017254	1.14	0.798
Itpr1	Inositol 1,4,5-triphosphate receptor, type 1	NM_001007235	1.36	0.131
Itpr2	Inositol 1,4,5-triphosphate receptor, type 2	NM_031046	0.73	0.034
Kras	V-Ki-ras2 Kirsten rat sarcoma viral oncogene homolog	NM_031515	1.21	0.266
Lpar1	Lysophosphatidic acid receptor 1	NM_053936	0.11	0.001
Map2k1	Mitogen activated protein kinase kinase 1	NM_031643	0.93	0.387
Map2k2	Mitogen activated protein kinase kinase 2	NM_133283	1.10	0.063
Map2k5	Mitogen activated protein kinase kinase 5	NM_017246	1.09	0.324

See published version at: https://doi.org/10.1007/s10571-020-00836-z

Map3k2	Mitogen activated protein kinase kinase kinase 2	NM_138503	1.33	0.100
Mapk1	Mitogen activated protein kinase 1	NM_053842	0.87	0.179
Mapk3	Mitogen activated protein kinase 3	NM_017347	0.66	0.009
Mapk7	Mitogen-activated protein kinase 7	NM_001191547	0.97	0.760
Nov	Nephroblastoma overexpressed gene	NM_030868	1.48	0.468
Nras	Neuroblastoma ras oncogene	NM_080766	0.74	0.002
Panx1	Pannexin 1	NM_199397	0.83	0.325
Panx2	Pannexin 2	NM_199409	1.96	0.159
Panx3	Pannexin 3	NM_199398	1.26	0.188
Pdgfra	Platelet derived growth factor receptor, alpha polypeptide	NM_012802	0.83	0.231
Pdgfrb	Platelet derived growth factor receptor, beta polypeptide	NM_031525	1.40	0.250
Plcb1	Phospholipase C, beta 1 (phosphoinositide-specific)	NM_001077641	0.87	0.161
Plcb2	Phospholipase C, beta 2	NM_053478	1.35	0.126
Plcb3	Phospholipase C, beta 3 (phosphatidylinositol-specific)	NM_033350	1.24	0.354
Plcb4	Phospholipase C, beta 4	NM_024353	1.02	0.835
Prkaca	Protein kinase, cAMP-dependent, catalytic, alpha	NM_001100922	0.97	0.580
Prkacb	Protein kinase, cAMP dependent, catalytic, beta	NM_001077645	0.88	0.099
Prkca	Protein kinase C, alpha	NM_001105713	0.81	0.256
Prkcb	Protein kinase C, beta	NM_012713	1.08	0.357
Prkcg	Protein kinase C, gamma	NM_012628	1.12	0.768
Prkg1	Protein kinase, cGMP-dependent, type 1	NM_001105731	0.94	0.885
Prkg2	Protein kinase, cGMP-dependent, type II	NM_013012	1.08	0.608
Raf1	V-raf-leukemia viral oncogene 1	NM_012639	0.86	0.041
Sos1	Son of sevenless homolog 1 (Drosophila)	NM_001100716	0.90	0.176
Sos2	Son of sevenless homolog 2 (Drosophila)	NM_001135561	0.78	0.019
Src	V-src sarcoma viral oncogene homolog	NM_031977	0.95	0.332
Tjap1	Tight junction associated protein 1	NM_001108203	0.80	0.292
Tjp1	Tight junction protein 1	NM_001106266	1.04	0.671
Tjp2	Tight junction protein 2	NM_053773	0.84	0.008
Tuba1a	Tubulin, alpha 1A	NM_022298	1.02	0.863
Tuba1c	Tubulin, alpha 1C	NM_001011995	1.01	0.923
Tuba3a	Tubulin, alpha 3A	NM_001040008	1.41	0.174
Tuba4a	Tubulin, alpha 4A	NM_001007004	1.37	0.357
Tubb2b	Tubulin, beta 2b	NM_001013886	0.78	0.087
Tubb4b	Tubulin, beta 2c	NM_199094	0.98	0.838
Tubb3	Tubulin, beta 3	NM_139254	0.88	0.206
Tubb4a	Tubulin, beta 4	NM_080882	0.44	0.029
Tubb5	Tubulin, beta 5	NM_173102	0.98	0.753
Tubb6	Tubulin, beta 6	NM_001025675	1.49	0.141
Tubd1	Tubulin, delta 1	NM_001105826	1.02	0.853
Tube1	Tubulin, epsilon 1	NM_001108536	1.10	0.366
Tubg1	Tubulin, gamma 1	NM_145778	1.29	0.001